Neuroimage: Reports 2 (2022) 100082

Contents lists available at ScienceDirect

Neuroimage: Reports

journal homepage: www.sciencedirect.com/journal/neuroimage-reports

# Impact of prenatal alcohol exposure on intracortical myelination and deep white matter in children with attention deficit hyperactivity disorder

Lisa A. Kilpatrick [a,*], Jeffry R. Alger [b,e,f], Joseph O'Neill [c], Shantanu H. Joshi [b,g], Katherine L. Narr [b,d], Jennifer G. Levitt [c], Mary J. O'Connor [c]

[a] G. Oppenheimer Family Center for Neurobiology of Stress and Resilience, Vatche and Tamar Manoukian Division of Digestive Diseases, David Geffen School of Medicine at University of California, Los Angeles, CA, USA
[b] Department of Neurology, University of California, Los Angeles, CA, USA
[c] Division of Child & Adolescent Psychiatry, Jane & Terry Semel Institute for Neuroscience, University of California Los Angeles, CA, USA
[d] Department of Psychiatry and Biobehavioral Sciences, University of California, Los Angeles, CA, USA
[e] Neurospectroscopics, LLC., Sherman Oaks, CA, USA
[f] Advanced Imaging Research Center, University of Texas Southwestern Medical Center, Dallas, TX, USA
[g] Department of Bioengineering, University of California, Los Angeles, CA, USA

ARTICLE INFO

*Keywords:*
Attention deficit hyperactivity disorder
Fetal alcohol spectrum disorders
Myelination
Diffusion-weighted magnetic resonance imaging
Prenatal alcohol exposure

ABSTRACT

White matter alterations have been reported in children with prenatal alcohol exposure (PAE) and in children with attention deficit hyperactivity disorder (ADHD); however, as children with PAE often present with ADHD, covert PAE may have contributed to previous ADHD findings. Additionally, data regarding intracortical myelination in ADHD are lacking. Therefore, we evaluated intracortical myelination (assessed as the T1w/T2w ratio at 4 cortical ribbon levels) and myelin-related deep white matter features in children (aged 8–13 years) with ADHD with PAE (ADHD + PAE), children with familial ADHD without PAE (ADHD-PAE), and typically developing (TD) children. In widespread tracts, ADHD + PAE children showed higher mean and radial diffusivity than TD and ADHD-PAE children and lower fractional anisotropy than ADHD-PAE children; ADHD-PAE and TD children did not differ significantly. Compared to TD children, ADHD + PAE children had lower intracortical myelination only at the deepest cortical level (mainly in right insula and cingulate cortices), while ADHD-PAE children had lower intracortical myelination at multiple cortical levels (mainly in right insula, sensorimotor, and cingulate cortices); ADHD + PAE and ADHD-PAE children did not differ significantly in intracortical myelination. Considering the two ADHD groups jointly (via non-parametric combination) revealed common reductions in intracortical myelination, but no common deep white matter abnormalities. These results suggest the importance of considering PAE in ADHD studies of white matter pathology. ADHD + PAE may be associated with deeper, white matter abnormalities, while familial ADHD without PAE may be associated with more superficial, cortical abnormalities. This may be relevant to the different treatment response observed in these two ADHD etiologies.

## 1. Introduction

Animal models have detailed long-lasting deleterious effects of prenatal alcohol exposure (PAE) on myelination. For example, PAE in rats reduces expression of mRNA of myelin basic protein and of a myelin-specific enzyme (2',3'-cyclic nucleotide 3'-phosphodiesterase) in offspring throughout the entire developmental period (Bichenkov and Ellingson, 2001, 2002; Kojima et al., 1994). Expression of transferrin, thought to play an important role in myelinogensis, is also reduced (Chiappelli et al., 1991). Furthermore, PAE substantially affects the number and morphology of oligodendrocytes, but not of astrocytes, and alters the composition of the myelin sheath (Bichenkov and Ellingson, 2009; Chiappelli et al., 1991). As the turnover rate of myelin components in already formed axon sheaths is extremely low, abnormal myelin composition is difficult to repair. Thus, animal models suggest that PAE targets oligodendrocytes, resulting in delayed maturation and long-lasting changes in myelination. Consistent with this, numerous studies have reported abnormal diffusion tensor imaging (DTI) indices

* Corresponding author. Oppenheimer Family Center for Neurobiology of Stress and Resilience University of California, Los Angeles, CHS 42-210 MC737818 10833 Le Conte Avenue, CA, 90095, USA.
*E-mail addresses:* lakilpatrick@ucla.edu, lakilpatrick@mednet.ucla.edu (L.A. Kilpatrick).

https://doi.org/10.1016/j.ynirp.2022.100082
Received 31 August 2021; Received in revised form 4 January 2022; Accepted 11 January 2022
Available online 18 January 2022

in deep white matter in children with PAE (Ghazi Sherbaf et al., 2019; Taylor et al., 2015).

Deep white matter alterations have also been reported in children with attention deficit hyperactivity disorder (ADHD), which have been attributed to delayed myelination (Aoki et al., 2018; Chen et al., 2016). Furthermore, genetic linkage and association studies have revealed associations between ADHD and genes that impact oligodendrocyte function and myelin formation, maintenance, and repair (e.g., fibroblast growth factor and sphingolipid metabolism genes) (Henriquez-Henriquez et al., 2020; Lesch, 2019; Mastronardi et al., 2016; Puentes-Rozo et al., 2019). Thus, disruptions in myelination may be involved in ADHD. However, a recent review and meta-analysis of DTI studies on ADHD noted substantial variation among studies, and found that of the 6 studies that had no significant between-group differences in head motion, which can influence DTI results, 4 found no significant differences between ADHD and typically developing (TD) individuals in DTI metrics (Aoki et al., 2018). Furthermore, although children with PAE typically exhibit ADHD symptoms, underlying PAE is often unrecognized in diagnosing ADHD (Fryer et al., 2007; O'Connor, 2014; O'Malley and Nanson, 2002). Thus, covert PAE may have contributed to the reported white matter pathology in some ADHD studies. Consistent with this, in our recently published analysis of fractional anisotropy (FA, a summary measure of microstructural integrity) in the anterior corona radiatae, we found lower FA associated with PAE regardless of ADHD status (i.e., a main effect of PAE), but no effect of ADHD (O'Neill et al., 2019). As treatment response to ADHD medications differs between patients with and without PAE (Doig et al., 2008; Frankel et al., 2006; Oesterheld et al., 1998; Peadon et al., 2009; Snyder et al., 1997), a better understanding of the white matter pathology associated with PAE in ADHD may improve treatment.

Although myelin is a prominent deep white matter component, the cerebral cortex also contains a significant number of myelinated fibers. Unlike deep white matter, myelination patterns in the cortex are highly complex, varying between cortical regions and layers, and showing discontinuity (Mazuir et al., 2021; Micheva et al., 2016; Tomassy et al., 2014). Cortical myelin has long been known to ensheath excitatory axons connecting to subcortical nuclei and other remote cortices; however, a large fraction of myelin in cortical layers 1–3 ensheaths the axons of inhibitory neurons (specifically parvalbumin-positive basket cells) (Micheva et al., 2016, 2018; Stedehouder et al., 2017). In cortical deeper layers, although myelinated inhibitory GABA interneurons are also found, the proportion of non-GABA myelinated axons is greatly increased (Micheva et al., 2018). The course of intracortical myelination is protracted in humans, especially in the prefrontal cortex (Norbom et al., 2020; Yakovlev and Lecours, 1967). As these regions also exhibit protracted functional changes, intracortical myelination is thought to play an important role in multiple aspects of neurodevelopment (Deoni et al., 2015; Grydeland et al., 2013; Natu et al., 2018). However, the impact of PAE on intracortical myelination and its role in ADHD remain unclarified.

In this investigation, we used advanced MRI techniques to evaluate intracortical myelination and myelin-related deep white matter features in children (aged 8–13 years) with ADHD, with and without PAE ("ADHD + PAE" and "ADHD-PAE", respectively), compared to those in TD children. In recent work, we found lower cortical gyrification in both ADHD + PAE and ADHD-PAE children than in TD children, with some regional differences between the two ADHD etiologies (Kilpatrick et al., 2021). We further found that multi-modal imaging of deep white matter combined with ADHD symptom profiling could accurately classify individual patients as ADHD + PAE vs. ADHD-PAE (O'Neill et al., 2021). Here, we hypothesized that, although there may be myelination alterations common to the two ADHD groups, children with ADHD + PAE would show unique or more severe alterations.

## 2. Methods and materials

### 2.1. Participants

This study was approved by our Institutional Review Board; written informed assent/consent was obtained from all participants. Children aged 8–13 years were recruited from community organizations, FASD parent organizations, national websites, other pediatric research studies, or physician referrals from local child psychiatry or pediatric clinics.

Children in the ADHD + PAE group met DSM-5 criteria for ADHD (any subtype) according to the clinician-administered computerized Schedule for Affective Disorders and Schizophrenia for School Aged Children, Parent Version (K-SADS) (Kaufman et al., 1997; Townsend et al., 2020) and the Conners-3 Parent Form (Conners, 2008); had diagnostic features of fetal alcohol syndrome (FAS), partial fetal alcohol syndrome (pFAS), or alcohol-related neurodevelopmental disorder (ARND) according to the Institute of Medicine (IOM) criteria proposed in updated guidelines (Hoyme et al., 2016; O'Connor et al., 2019); and had a clear history of PAE ($\geq$6 drinks/week for $\geq$2 weeks and/or $\geq$3 drinks on $\geq$2 occasions including the time periods prior to and following pregnancy recognition). The diagnostic features of FAS comprised growth retardation; presence of the FAS facial phenotype, including short palpebral fissures, flat philtrum, and flat upper vermillion border (Hoyme et al., 2016); neurodevelopmental dysfunction; and gestational alcohol exposure. The criteria for a history of PAE are based on findings that $\geq$6 drinks/week is an adequate measure of exposure for an FASD, and on epidemiologic studies demonstrating adverse fetal effects of episodic drinking of $\geq$3 drinks per occasion (Hoyme et al., 2016).

Children in the ADHD-PAE group met ADHD criteria (as defined above), had at least one first-degree family member (i.e., biological parent or sibling) diagnosed with ADHD, and had PAE of <2 standard drinks (1.20 oz absolute alcohol) during gestation. Familial ADHD without PAE was selected as a homogeneous ADHD-PAE comparison group with a well-defined ADHD etiology.

Typically developing children (TD group) had no current or lifetime history of an Axis I mental disorder by K-SADS interview and PAE of <2 standard drinks during gestation.

Exclusion criteria for all participants were as follows: estimated Full-Scale IQ <70 on the Wechsler Abbreviated Scale of Intelligence, Second Edition (WASI-II) (Wechsler, 2011); known genetic syndrome associated with ADHD, including fragile X, tuberous sclerosis, and generalized resistance to thyroid hormone; pervasive developmental disorder; serious medical or neurologic illness likely to influence cognition or brain function or brain anatomy (e.g., a seizure disorder or history of closed-head trauma); gestation <34 weeks; history of claustrophobia; ferromagnetic metal implant, braces, or other contraindication to MRI; primary language at home was not English; unable to comply with study procedures; or poor imaging scan quality. Additionally, as prenatal methamphetamine exposure has been reported to show effects on DTI measures opposite to those seen with PAE alone (Colby et al., 2012), children with prenatal methamphetamine/amphetamine exposure were excluded.

Prenatal exposures were determined using the Health Interview for Women (HIW), which assesses the frequency and quantity of typical and binge drinking and use of other teratogens prior to and following recognition of pregnancy; or the Health Interview for Adoptive and Foster Parents (HIAFP) (Quattlebaum and O'Connor, 2013). For adopted/fostered participants, data regarding prenatal exposure to alcohol and other teratogens were obtained via birth, medical, or adoption records, or by reliable informants. As many individuals with FASD are adopted or fostered, this approach is often necessary, and is considered acceptable for establishing PAE by the scientific community (CDC, 2004). Although alcohol use was measured retrospectively, studies show that recall regarding drinking during pregnancy, predicts neurodevelopmental outcomes up to 14 years post-delivery (Hannigan et al., 2010).

### 2.2. Neuroimaging acquisition and analysis

Participants underwent extensive desensitization and training in keeping the head and other body parts still prior to MRI scanning. During scanning, participants watched a children's movie of their choice and were monitored via video feed from within the MRI unit; participants were reminded to hold still when motion was detected. Pulse sequences from the Human Connectome Project (HCP; https://www.humanconnectome.org/storage/app/media/documentation/s1200/HCP_S1200_Release_Appendix_I.pdf), as set in 2016, were used. Images were collected using a 3T Prisma-fit system (Siemens, Erlangen, Germany) with a 32-channel head coil at the UCLA Ahmanson Lovelace Brain Mapping Center. T1-weighted (T1w) imaging, T2-weighted (T2w) imaging and diffusion tensor imaging (DTI) were acquired with custom pulse-sequences and parameters prepared at the University of Minnesota for the Human Connectome Project. Magnetization-prepared rapid gradient-echo (MP-RAGE) 3-dimensional T1w imaging was performed using a sagittal multi-echo method that included real-time motion correction (TR/TEs/TI = 2500/1.81, 3.6, 5.39, 7.18/1000 ms; flip 8°; voxel dimensions 0.8 x 0.8 × 0.8 $mm^3$). This acquisition produced a T1w 3-dimensional image that was used for positioning of subsequent imaging, tissue-segmentation, and radiologic review. Subsequently a 3-dimensional T2w image was acquired with TR/TE = 3200/564 ms. The T2w image prescription was identical to that used for the T1w image acquisition. DTI was performed in four blocks using multiband accelerated multislice spin-echo echo-planar imaging (TR/TE = 3230/89.2 ms; b = 0, 1500, 3000 s/$mm^2$; 92 slices; voxel dimensions 1.5 x 1.5 × 1.5 $mm^3$; multiband factor 4; genu-splenium parallel slicing; whole-brain coverage with 98 or 99 b = 0 or diffusion-weighting directions). Two of the blocks used anterior-to-posterior echo planar imaging phase encoding and two used posterior-to-anterior phase encoding.

T1w and T2w images were processed using the Human Connectome Project (HCP) pipeline(Glasser et al., 2013). Briefly, volume segmentation and cortical surface reconstruction were performed with FreeSurfer version 6.0 (http://surfer.nmr.harvard.edu) (Dale et al., 1999), generating white and pial surfaces at the gray/white matter boundary and gray/cerebrospinal fluid boundary, respectively. In the present study, FreeSurfer surfaces were manually corrected as necessary. These surfaces were used to define the cortical ribbon and were registered to the HCP standard mesh. The T2w image was spatially-aligned to the T1w image and the ratio of T1w to T2w image intensity within the cortical ribbon was calculated. To support a fine-grained analysis, we evaluated the T1w/T2w ratio at multiple levels within the cortical ribbon using the -surface-cortex-layer command (in workbench 1.5.0 from the HCP; ttps://github.com/Washington-University/workbench). Specifically, we evaluated the T1w/T2w ratio at increments of 0.05 from 0.05 (i.e., 5% of the cortical thickness, near the white matter surface) to 1 (i.e. 100% of the cortical thickness, at the pial surface) and averaged over 5 consecutive increments to create 4 values per vertex, roughly reflecting deep cortical layers (average of the values at 5%–25% of the cortical thickness), lower- and upper-middle cortical layers (average at 30%–50% and 55%–75%, respectively), and upper cortical layers (average at 80%–100%).

DTI data that passed quality control (Section 2.3) were processed using FSL (http://fsl.fmrib.ox.ac.uk/fsl/fslwiki/), including distortion correction by topup and eddy, brain extraction by BET, and diffusion tensor model fitting by DTIFIT (Andersson et al., 2003, 2016; Behrens et al., 2003; Smith, 2002). A Tract-Based Spatial Statistics (TBSS) approach (Smith et al., 2006) was used to investigate diffusivity parameters in white matter tracts, including FA, mean diffusivity (MD), axial diffusivity (AD), and radial diffusivity (RD). DTIFIT directly produced FA and MD maps; AD and RD maps were determined from the eigenvalues produced by DTIFIT (with AD as λ1 and RD as the average of λ2 and λ3). These maps were nonlinearly aligned to Montreal Neurological Institute 152 (MNI) space and a study-specific white matter skeleton was created from the FA maps of all participants, with a FA threshold of 0.2. For each DTI metric, individual subjects' values were projected onto the group white matter skeleton. For ease in the implementation of analyses, the MD and RD maps were multiplied by −1 (creating negMD and negRD maps, respectively). Thus, lower values indicated greater abnormality (i.e., greater departure from the expected healthy state) for all analyzed DTI metrics.

### 2.3. Quality control

For T1w and T2w scans, image quality was evaluated using MRIQC (Esteban et al., 2017). The MRIQC reports indicated outliers in in the white matter signal-to-noise ratio (especially in the T2w scan) and quality index 1 (Qi1), which reflects the proportion of voxels with intensity corrupted by artifacts normalized by the number of voxels in the background; the vast majority of these participants did not show the expected overall myelination pattern (highest in visual cortex). Thus, a threshold for the white matter signal-to-noise ratio was established based on the distribution and participants with extreme values (<6) were excluded. Additionally, previously published thresholds for the Qi1 (Mortamet et al., 2009), which were established using data with a different protocol but appeared to be reasonable for the current data, were utilized; participants with a Qi1 exceeding 0.00506 or 0.0030 for T1w and T2w images, respectively, were excluded.

DTI quality control was performed as follows. For each subject study, the DTI acquisition produced 394 3-dimensional volumes of spin-echo echo-planar not-diffusion-weighted and diffusion-weighted signal intensity. Each of these volumes was comprised of 92 2-dimensional slices. Each 2-dimensional slice in each volume was visually inspected by an MRI expert (JRA). Visual inspection was aided by a custom-written software tool that displayed a volume of 2-dimensional signal intensity images in mosaic format and allowed the user to rapidly scroll through each of volumes that made up a particular acquisition. Studies that showed excessive B0-inhomogenity as low spatial-frequency signal intensity variation were tagged as quality control (QC) failures. In addition, there were volumes that showed one or more 2-dimensional slices that displayed partial or complete signal intensity loss that was likely due to subject motion or to scanner instability. Studies that showed excessive loss of signal intensity in individual slices over multiple volumes were tagged as QC failures. We also calculated traditional 3-dimensional color maps that displayed white matter fiber orientation using red-blue-green shading from all 394 3-dimensional signal intensity volumes for each subject. Color maps that displayed excessive blur (likely due to subject movement or scanner instability) during the entire DTI acquisition were tagged as QC failures. We confirmed that, after excluding participants with poor image quality, head motion during the DTI scan, as assessed by the average absolute and relative root-mean-square of the displacement, did not differ among the 3 groups (absolute: $F(2,65) = 0.23$, $p = 0.76$; relative: $F(2,65) = 1.89$, $p = 0.16$).

### 2.4. Statistical analysis

Group differences in demographic and clinical characteristics were evaluated by analyses of variance (ANOVAs) for continuous variables and by the chi-square test for categorical variables using SPSS v26 (IBM Corp., Armonk, NY).

Joint and individual differences in the 4 DTI parameters (FA, AD, negMD, negRD) between the groups were evaluated using non-parametric combination (NPC), implemented in the Permutation Analysis of Linear Models (PALM) toolbox in FSL (using the –npcmod flag), with 5000 permutations, threshold-free cluster enhancement, and family-wise error (FWE) correction for multiple comparisons, and controlling for sex and age (Smith and Nichols, 2009; Winkler et al., 2014). NPC combines the test statistics of separate (even if not independent) analyses into a single, joint statistic, the significance of which is assessed through synchronized permutations for each of the separate tests (Winkler et al., 2014, 2016). NPC has advantages over classical analyses

such as multivariate analysis of covariance in terms of assumptions and the ability to investigate the direction of joint effects, while simultaneously correcting across tests (Winkler et al., 2014, 2016). The primary comparisons comprised simple pairwise contrasts in the hypothesized direction (TD > ADHD + PAE, TD > ADHD-PAE, and ADHD-PAE > ADHD + PAE).

Group differences in intracortical myelination at 4 cortical levels (deep, lower-middle, upper-middle, upper) were also evaluated using the PALM toolbox in FSL with 5000 permutations, threshold-free cluster enhancement, FWE correction for multiple comparisons, and controlling for sex and age. However, separate analyses were conducted for each cortical level because, unlike the DTI parameters which had spatial concordance, the cortical levels used different surfaces, with different vertex areas, for threshold-free cluster enhancement. The primary comparisons comprised simple pairwise contrasts in the hypothesized direction (TD > ADHD + PAE, TD > ADHD-PAE, and ADHD-PAE > ADHD + PAE).

Additional NPC analyses were performed to determine alterations common to the two ADHD groups. Specifically, alterations in DTI metrics and intracortical myelination in the two ADHD groups (ADHD + PAE, ADHD-PAE) considered jointly were tested, controlling for sex and age, using the–npcccon flag, 5000 permutations, threshold-free cluster enhancement, FWE correction for multiple comparisons, and the following contrasts: TD > ADHD + PAE, TD > ADHD-PAE.

P-values <0.05 (FWE-corrected for imaging data) were considered significant.

## 3. Results

### 3.1. Participant characteristics

In total, 66 participants (ADHD + PAE: 22; ADHD-PAE: 20; TD: 24) were included in the DTI analysis and 71 participants (ADHD + PAE: 24; ADHD-PAE: 22; TD: 25) were included in the intracortical myelination analysis, with 58 participants (ADHD + PAE: 19; ADHD-PAE: 17; TD: 22) contributing to both analyses. We analyzed all data, rather than limiting the analysis to only those with useable data in both modalities, to maximize the sample sizes. Demographic and clinical data are summarized in Table 1. For both the DTI and intracortical myelination analyses, the groups did not differ in terms of demographic characteristics. Although IQ was significantly lower in the ADHD + PAE group than in the other groups, we did not include IQ as a covariate in the analyses, as this can lead to overcorrected, anomalous, and counterintuitive finding in studies of neurodevelopmental disorders (Dennis et al., 2009).

### 3.2. Deep white matter alterations

The NPC analysis of the two ADHD groups considered jointly did not reveal any significant common alterations in any of the DTI metrics. The NPC analysis of group differences across all DTI metrics revealed significant alterations in the ADHD + PAE group compared to the TD and ADHD-PAE groups in widespread tracts (Fig. 1). The partial tests revealed significantly lower negMD and negRD (as well as a trend for lower FA) in the ADHD + PAE than in the TD group, and significantly lower FA, negMD, and negRD in the ADHD + PAE group than in the ADHD-PAE group, in widespread tracts (Fig. 1). In general, the spatial extent of the reduction in the ADHD + PAE group was greater when compared to ADHD-PAE group than when compared to the TD group.

### 3.3. Intracortical myelination alterations

The NPC analysis of the two ADHD groups considered jointly revealed common reductions in intracortical myelination compared to that in the TD group at multiple cortical levels, from the deepest level to the upper-middle level (Fig. 2; Table 2). The group difference analysis revealed significantly lower intracortical myelination in the ADHD + PAE group than in the TD group at only the deepest cortical level, mainly in the right insula and anterior cingulate; these regions showed only trend-level p-values at middle cortical levels (Fig. 2; Table 2). In contrast, the ADHD-PAE group showed lower intracortical myelination compared to that in the TD group at multiple cortical levels, from the deepest level to the upper-middle level (Fig. 2; Table 2). However, the direct comparison between the ADHD + PAE and ADHD-PAE groups did not reveal any significant differences in intracortical myelination at any cortical level.

## 4. Discussion

The present study evaluated intracortical myelination (using the T1w/T2w ratio) and deep white matter abnormality (using the DTI metrics, FA, MD, AD, RD) in preadolescent children with ADHD + PAE or familial ADHD-PAE, compared to TD children. The DTI results demonstrated widespread white mater abnormality specific to the ADHD + PAE group, supporting our hypothesis of unique alterations in children with ADHD + PAE. In contrast, the intracortical myelination results generally supported common alterations in ADHD + PAE and ADHD-PAE, with some evidence of more widespread effects in ADHD-PAE.

The ADHD + PAE group had lower FA and higher MD and RD (i.e.,

**Table 1**
Demographic and clinical characteristics.

| | Diffusion tensor imaging | | | | Intracortical myelination | | | |
|---|---|---|---|---|---|---|---|---|
| | ADHD + PAE | ADHD-PAE | TD | P | ADHD + PAE | ADHD-PAE | TD | p |
| N | 22 | 20 | 24 | | 24 | 22 | 25 | |
| Male Sex, N (%) | 12(54.5) | 13(65.0) | 13(54.2) | 0.72 | 13(54.2) | 14(63.6) | 13(52.0) | 0.70 |
| Age, yrs | 9.7 ± 0.3 | 10.6 ± 0.3 | 10.5 ± 0.3 | 0.11 | 9.7 ± 0.3 | 10.3 ± 0.3 | 10.4 ± 0.3 | 0.16 |
| Race/ethnicity, N (%) | | | | 0.12‡ | | | | 0.10‡ |
| White | 5(22.7) | 13(65.0) | 11(45.8) | | 8(33.3) | 15(68.2) | 11(44.0) | |
| Black | 4(18.2) | 1(5.0) | 0(0) | | 2(8.3) | 1(4.5) | 0(0) | |
| Latino | 5(22.7) | 2(10.0) | 7(29.2) | | 6(25.0) | 1(4.5) | 7(28.0) | |
| Asian | 1(4.5) | 2(10.0) | 2(8.3) | | 1(4.42) | 3(13.6) | 3(12.0) | |
| Other | 1(4.5) | 0(0) | 1(4.2) | | 0(0) | 0(0) | 1(4.0) | |
| Mixed | 6(27.3) | 2(10.0) | 3(12.5) | | 7(29.2) | 2(9.1) | 3(12.0) | |
| Mother's education, yrs | 15.8 ± 0.4 | 16.7 ± 0.8 | 17.2 ± 1.0 | 0.46 | 16.1 ± 0.4 | 17.0 ± 0.8 | 17.7 ± 1.1 | 0.39 |
| Full-scale IQ | 97.3 ± 3.0*† | 108.6 ± 2.8 | 116.0 ± 3.3 | <0.001 | 98.4 ± 2.8*† | 108.7 ± 2.8 | 112.8 ± 3.3 | 0.003 |
| Inattention | 81.5 ± 2.2* | 83.0 ± 1.8* | 48.3 ± 2.1 | <0.001 | 83.7 ± 1.9* | 82.1 ± 2.1* | 48.0 ± 2.0 | <0.001 |
| Hyperactivity/impulsivity | 84.1 ± 1.7* | 79.3 ± 2.9* | 50.3 ± 2.4 | <0.001 | 83.8 ± 1.8* | 80.0 ± 2.7* | 49.5 ± 2.4 | <0.001 |

Mother's education is a proxy for socioeconomic status. Inattention and hyperactivity/impulsivity as assessed by the Conners-3.
*p<0.05 ADHD+/-PAE vs TD; †p<0.05 ADHD + PAE vs ADHD-PAE; ‡ Pearson chi-square exact significance was computed due to the number of cells with low values; ADHD, attention deficit hyperactivity disorder; PAE, prenatal alcohol exposure; TD, typically developing.

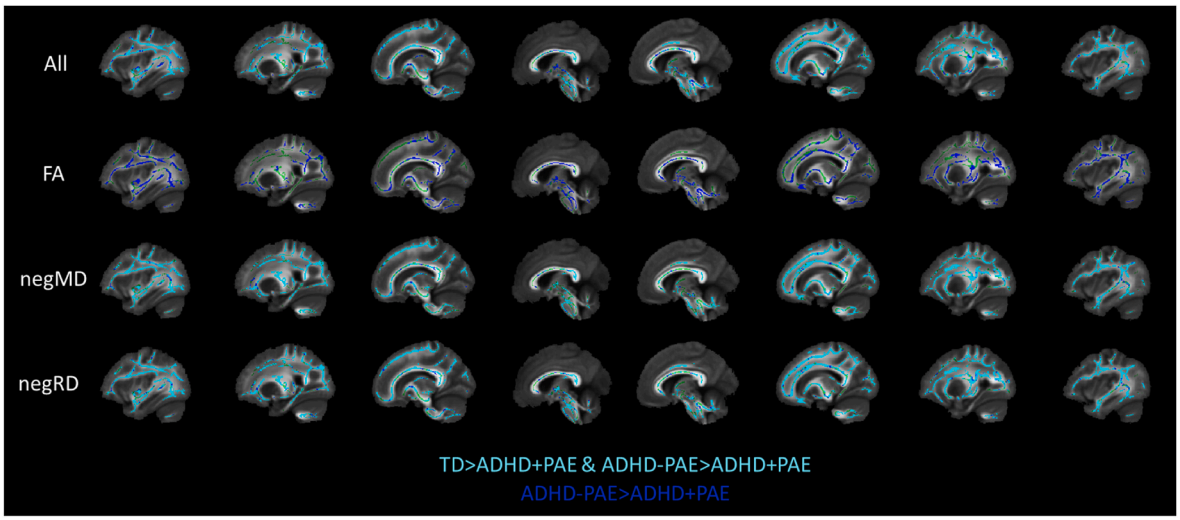


**Fig. 1.** Reduced deep white matter DTI metrics in children with ADHD + PAE compared to that in children with ADHD-PAE and TD children. The ADHD + PAE group showed significant ($p_{fwe}<0.05$) reductions in all DTI metrics considered jointly (All), fractional anisotropy (FA), negative mean diffusivity (negMD; reverse coded for ease in presentation), and negative radial diffusivity (negRD) compared to those in the ADHD-PAE and TD groups (with the exception of FA). The mean FA skeleton is shown in green. Voxels with significance on both TD > ADHD + PAE and ADHD-PAE > ADHD + PAE are shown in cyan; voxels with significance on ADHD-PAE > ADHD + PAE only are shown in dark blue. ADHD, attention deficit hyperactivity disorder; PAE, prenatal alcohol exposure; TD, typically developing; DTI, diffusion tensor imaging.

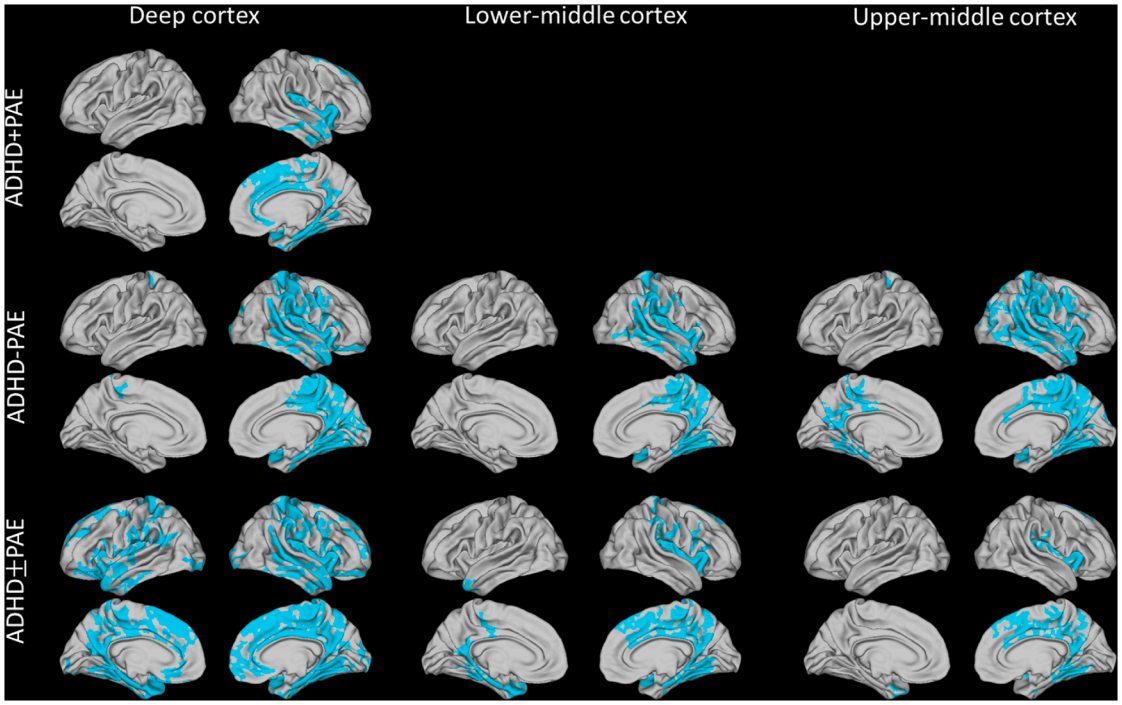


**Fig. 2.** Intracortical myelination reductions in children with ADHD + PAE and with ADHD-PAE compared to TD children. The ADHD + PAE and ADHD-PAE groups considered jointly (ADHD ± PAE) showed significantly ($p_{fwe}<0.05$) reduced myelination in the deep (5–25% of the cortical thickness from the white-gray boundary), lower-middle (30–50% of the cortical thickness from the white-gray boundary), lower-upper cortical layers (55–75% of the cortical thickness from the white-gray boundary). When compared against TD children separately, the ADHD-PAE group showed more spatially extensive reduction in myelination than the ADHD + PAE group. ADHD, attention deficit hyperactivity disorder; PAE, prenatal alcohol exposure; TD, typically developing.

lower negMD and negRD) than the ADHD-PAE group, and higher MD and RD than the TD group. These changes are consistent with the generally known effects of disrupted myelination (low myelination, demyelination, delayed maturation) on FA (decreased), MD (increased), and RD (increased) (Feldman et al., 2010). Furthermore, the results are consistent with previous studies comparing deep white matter integrity between children with PAE and TD children, which have most consistently shown abnormality in the corpus callosum and cerebellar peduncles, followed by the cingulum (Ghazi Sherbaf et al., 2019). The current study adds to this literature by showing that PAE-related reductions are also seen in the context of ADHD. In fact, the differences between the ADHD + PAE and ADHD-PAE groups were more striking than those between the ADHD + PAE and TD groups, especially for FA.

Although numerous DTI studies have reported abnormalities in

**Table 2**
Clusters showing significant differences in intracortical myelination between groups.

| | Peak | X | Y | Z | Size $mm^2$ | FWE-corrected p-value |
|---|---|---|---|---|---|---|
| ADHD + PAE < TD | | | | | | |
| *Deepest cortical level (5%-25%)* | | | | | | |
| **Cluster 1** | R_PHA3 (temporal) | 37.1 | −25.6 | −21.6 | 58906 | 0.034 |
| **temporal** | R_Pir | 39.9 | 1.7 | −23.4 | 2093 | |
| **occipital** | R_TF | 39.7 | −25.4 | −23.6 | 686 | |
| **insula** | R_AAIC | 36.3 | 12.1 | −7.0 | 2930 | |
| **frontal** | R_SCEF | 10.1 | 15.1 | 49.4 | 1736 | |
| | R_SCEF | 10.7 | 12.8 | 48.7 | 2934 | |
| **cingulate** | R_POS1 | 13.2 | −55.7 | 18.6 | 601 | |
| **parietal** | R_23c | 13.9 | −24.2 | 36.8 | 568 | |
| ADHD-PAE < TD | | | | | | |
| *Deepest cortical level (5%-25%)* | | | | | | |
| **Cluster 1** | L_5m (parietal) | −11.1 | −32.8 | 51.0 | 319 | 0.049 |
| **Cluster 2** | L_2 (parietal) | −21.3 | −36.8 | 61.6 | 200 | 0.049 |
| **Cluster 3** | L_5L (parietal) | −16.0 | −42.1 | 74.0 | 124 | 0.049 |
| **Cluster 4** | R_Mbelt (temporal) | 35.9 | −27.6 | 9.4 | 35778 | 0.016 |
| **temporal** | R_Pir | 36.0 | 1.5 | −23.2 | 4719 | |
| | R_VMV3 | 31.6 | −58.2 | −5.9 | 2827 | |
| | R_A1 | 38.9 | −26.2 | 9.3 | 809 | |
| | R_ProS | 14.6 | −46.3 | 1.2 | 4498 | |
| **insula** | R_4 | 23.1 | −22.7 | 55.9 | 4321 | |
| **frontal** | R_AAIC | 30 | 13.9 | −12.9 | 1105 | |
| | R_PreS | 12.9 | −42.8 | 1.2 | 1458 | |
| **cingulate** | R_PFcm | 44.7 | −25.6 | 21.1 | 9255 | |
| **parietal** | R_V3 | 11.6 | −88.7 | 19.3 | 765 | |
| *Lower-middle (30%-50%)* | | | | | | |
| **Cluster 1** | R_V2 (occipital) | 12.1 | −65.7 | 14.0 | 106 | 0.049 |
| **Cluster 2** | R_PoI1 (insula) | 34.7 | −17.9 | 5.9 | 12628 | 0.033 |
| **Cluster 3** | R_VMV2 (temporal) | 22.6 | −60.5 | −7.0 | 11993 | 0.043 |
| *Upper-middle (55%-75%)* | | | | | | |
| **Cluster 1** | L_24dd (frontal) | −10.2 | −30.5 | 49.6 | 5436 | 0.049 |
| **Cluster 2** | L_5L (parietal) | −13.6 | −40.7 | 68.6 | 250 | 0.048 |
| **Cluster 3** | L_2 (parietal) | −20.6 | −38.5 | 60.6 | 112 | 0.049 |
| **Cluster 4** | R_RI (insula) | 35.5 | −32 | 20.7 | 37207 | 0.016 |
| **temporal** | R_MBelt | 41.0 | −24.5 | 7.4 | 6323 | |
| | R_VMV2 | 31.2 | −58.3 | −5.4 | 2282 | |
| **occipital** | R_VMV1 | 21.2 | −61.2 | −7.1 | 2434 | |
| | R_PGs | 37.2 | −76.4 | 33.1 | 944 | |
| | R_MST | 45.0 | −61.1 | 3.1 | 627 | |
| **frontal** | R_OP1 | 42.1 | −22.8 | 20.4 | 4583 | |
| | R_24dd | 9.8 | −22 | 49.6 | 526 | |
| **cingulate** | R_RSC | 12.8 | −46.7 | 2.4 | 2205 | |
| **parietal** | R_PFcm | 52.7 | −22.2 | 20.3 | 11856 | |
| ADHD ± PAE < TD | | | | | | |
| *Deepest cortical level (5%-25%)* | | | | | | |
| **Cluster 1** | R_6a (frontal) | 22.8 | 12.3 | 46.4 | 161 | 0.019 |
| **Cluster 2** | L_TGv (temporal) | −28.8 | 3.1 | −40.5 | 31462 | 0.048 |
| **temporal** | L_MBelt | −40.1 | −25.7 | 8.7 | 1188 | |
| **occipital** | L_V3 | −21.8 | −75.0 | −5.5 | 1984 | |
| | L_RSC | −10.6 | −50.5 | 5.1 | 525 | |
| **insula** | L_PI | −41.5 | −1.2 | −22.9 | 2708 | |
| **frontal** | L_SFL | −10.1 | 9.5 | 64.0 | 5729 | |
| | L_OFC | −16.0 | 16.9 | −21.4 | 2188 | |
| | L_PFcm | −53.4 | −24.1 | 21.4 | 1224 | |
| **cingulate** | L_RSC | −9.5 | −50.0 | 5.1 | 1790 | |
| | L_d32 | −12.4 | 37.4 | 13.9 | 631 | |
| **parietal** | L_POS1 | −13.5 | −58.8 | 11.5 | 4749 | |
| | L_PFop | −58.3 | −24.9 | 23 | 1149 | |
| **Cluster 3** | R_52 (insula) | 32.3 | −23.9 | 10.6 | 42757 | 0.016 |
| **temporal** | R_Pir | 37.2 | 1.8 | −23.1 | 7993 | |
| | R_A1 | 38.4 | −26.6 | 9.0 | 896 | |
| **occipital** | R_RSC | 14.0 | −46.2 | 1.4 | 4105 | |
| | R_TF | 39.7 | −26.0 | −23.4 | 896 | |
| **frontal** | R_OP1 | 44.7 | −24.4 | 21.0 | 3028 | |
| | R_9m | 10.3 | 53.8 | 6.3 | 2539 | |
| | R_24dd | 6.7 | −29 | 51.0 | 2335 | |
| | R_3a | 24.0 | −22.8 | 53.6 | 2116 | |
| | R_AAIC | 28.9 | 13.6 | −14.1 | 1351 | |
| **cingulate** | R_PreS | 12.7 | −43.3 | 1.1 | 3864 | |
| **parietal** | R_PFcm | 44.7 | −25.6 | 21.1 | 7019 | |
| | R_PF | 58.5 | −34.1 | 36.8 | 1409 | |
| *Lower-middle (30%-50%)* | | | | | | |
| **Cluster 1** | L_TGv (temporal) | −29.0 | 4.3 | −40.6 | 4602 | 0.042 |
| **Cluster 2** | R_PoI2 (insula) | 37.6 | 2.2 | −11.8 | 21495 | 0.033 |
| **temporal** | R_PHA3 | 37.2 | −24.3 | −22.8 | 2238 | |
| **occipital** | R_ProS | 15.0 | −46.2 | 0.9 | 938 | |
| **frontal** | R_3a | 34.3 | −25.8 | 45.5 | 1609 | |
| | R_SCEF | 10.1 | 15.1 | 49.4 | 1369 | |
| | R_FOP4 | 41.9 | 4.8 | 11.2 | 1320 | |
| **cingulate** | R_PreS | 13.9 | −44.8 | 0.3 | 2637 | |
| **parietal** | R_POS1 | 9.4 | −55.9 | 14.3 | 3705 | |
| | R_PFcm | 44.7 | −25.6 | 21.1 | 1650 | |
| *Upper-middle (55%-75%)* | | | | | | |
| **Cluster 1** | L_TGv (temporal) | −29.0 | 4.3 | −40.6 | 367 | 0.046 |
| **Cluster 2** | R_VMV2 (temporal) | 30.4 | −59.8 | −5.0 | 9249 | 0.036 |
| **Cluster 3** | R_PoI1 (insula) | 34.7 | −21.8 | 2.7 | 3877 | 0.036 |

For each cluster, the peak region (based on the HCPMMP1.0 atlas), peak coordinates (in MNI space), cluster size, and corrected p-value are provided. For extremely large clusters (>20,000 $mm^2$), subcluster information is provided. ADHD, attention deficit hyperactivity disorder; PAE, prenatal alcohol exposure; TD, typically developing.

ADHD vs TD, many of those with confirmed lack of significant head motion did not find differences between groups (Aoki et al., 2018). In the current study, we confirmed that there were no significant differences in head motion among the groups after performing stringent quality control. Under these conditions, and with a focus specifically on familial ADHD (i.e., no covert ADHD + PAE cases), we did not find any significant alterations in deep white matter tracts in ADHD-PAE (vs TD). Furthermore, there were no alterations common to ADHD-PAE and ADHD + PAE.

In contrast to the analysis on deep white matter integrity, the intracortical myelination analysis showed myelination disruptions in both ADHD + PAE and ADHD-PAE (vs TD). When the two ADHD groups were considered jointly, bilateral reductions in myelination at the deep cortical level (i.e., the deepest cortical layers), and predominately right-sided reductions in myelination at middle cortical levels, were observed. Additionally, there were no significant differences between the ADHD + PAE and ADHD-PAE groups, suggesting similar cortical myelin abnormalities in the two groups. However, when analyzed separately against the TD group, the ADHD + PAE and ADHD-PAE groups showed a difference in the robustness of the myelination disruptions observed in the joint analysis. In the ADHD + PAE vs TD comparison, only right-sided

reductions in myelination at the deep cortical level (mainly in insular, cingulate, and medial temporal regions) reached significance. In contrast, the ADHD-PAE group, compared to the TD group, showed significant reductions in myelination throughout most cortical levels, mainly involving insular, sensorimotor, posterior cingulate, and temporal cortical regions. These results may indicate that, in the affected regions, the ensheathment of axons in deep cortical layers (containing some GABA axons, but predominately comprising non-GABA axons, and largely impacting cortical-subcortical connectivity) (Micheva et al., 2016, 2018; Stedehouder et al., 2017) are impaired in both ADHD + PAE and ADHD-PAE. The fraction of cortical myelin ensheathing the axons of inhibitory neurons in layers 2/3 (mainly parvalbumin-positive basket cells, and largely impacting intercortical connectivity) (Micheva et al., 2016, 2018; Stedehouder et al., 2017) may also be disrupted in both ADHD + PAE and ADHD-PAE; however, the results were more robust in ADHD-PAE.

Alternatively, the number/density of cell populations typically myelinated, such as parvalbumin-positive interneurons, could be reduced. Consistent with this, several animal studies have found that PAE resulted in a reduced number/density of parvalbumin-positive interneurons, especially in the anterior cingulate cortex (Hamilton et al., 2017; Moore et al., 1998; Smiley et al., 2015). Parvalbumin-positive interneurons play an important role in excitatory/inhibitory balance in the cortex; fewer such interneurons could result in less inhibition on pyramidal cells, leading to over-excitation (Selten et al., 2018). Furthermore, axonal myelination of parvalbumin-positive interneurons might function in part to inhibit synapse formation along the proximal axon, potentially facilitating synchronous inhibition of postsynaptic targets (Stedehouder et al., 2017). Disruption of parvalbumin-positive interneurons during adolescence (a sensitive period) has been shown to lead to increased hyperactivity and impulsivity (Khan et al., 2017). Additionally, an animal study reported that PAE-related reduction in the number/density of parvalbumin-positive interneurons in the anterior cingulate cortex is associated with delayed learning of a passive avoidance task that requires behavioral flexibility and inhibitory control (Hamilton et al., 2017). Another animal study showed that medial prefrontal parvalbumin-positive interneurons are recruited by attentional processing and that elevated and sustained parvalbumin-positive interneuronal activity predicts the successful execution of goal-directed behavior (Kim et al., 2016). Thus, disruptions in parvalbumin-positive interneurons may contribute to ADHD symptomatology.

Furthermore, the results of DTI studies on ADHD have been used as a rationale for focused genetic studies (Henriquez-Henriquez et al., 2020). However, the current study results suggest that the impact of ADHD on white matter pathology is complicated and PAE must be considered. Additionally, intracortical myelination might be a more potent phenotype than deep white matter integrity in investigating the genetics of ADHD without the presence of PAE.

### 4.1. Limitations

The present study has limitations. The sample size was too small to examine the impact of sex and various epidemiological epiphenomena that may co-occur with PAE (e.g., neglect, maternal stress, etc.) However, the sample sizes were comparable to previous PAE and ADHD DTI studies (Aoki et al., 2018; Ghazi Sherbaf et al., 2019). All participants in our study had IQ >70. This criterion may have diluted differences between sample groups, as most studies of children with PAE include those from more extreme cases meeting the criteria for an intellectual disability. However, IQ >70 is more representative of the vast majority of children with developmental sequelae associated with PAE. On the one hand, this implies that our sample was more homogeneous; on the other hand, it means our results may not be extrapolated to the large category of children with low IQ and PAE. Our results also cannot be generalized to children with prenatal poly-drug exposures including both alcohol and methamphetamine, as methamphetamine exposure may have different (opposing) effects on DTI metrics than PAE alone (Colby et al., 2012). Regarding the MRI in our study, although the T1w/T2w ratio is a commonly used measure of intracortical myelination, it is an indirect measure (Glasser and Van Essen, 2011). Finally, the MRI spatial resolution in the current study allowed only a crude investigation of laminar differences. It is possible that the substantial reduction in the neighboring superficial white matter in the ADHD + PAE group contributed to the ADHD + PAE findings in the deeper cortical layers due to current limitations in partial-volume correction. Thus, results should be confirmed (e.g., at ultra-high field) and expanded upon in further studies with a similar design, but larger sample sizes and additional imaging acquisition protocols sensitive to intracortical myelination.

### 4.2. Conclusions

Present results suggest the importance of considering PAE in ADHD studies of white matter pathology. In the context of ADHD, PAE clearly reduces deep white matter integrity in many tracts, and may reduce intracortical myelination, especially in deeper cortical layers, during preadolescence. In contrast, familial ADHD, without PAE, does not appear to impact deep white matter integrity, but reduces intracortical myelination at multiple cortical levels, potentially affecting different cell populations and the coordination of a wider range of connections (cortico-subcortical and cortico-cortical) during preadolescence. In a modification of Carlsson et al.'s (1999) model, we proposed that there are separate "gray matter" and "white matter" paths to ADHD, characteristic of ADHD-PAE and ADHD + PAE, respectively (O'Neill et al., 2021). Present findings revealing greater deep white matter abnormalities in ADHD + PAE and more robust cortical abnormalities in ADHD-PAE are consistent with this picture. These results may further support the need for different treatment strategies for children with and without PAE.

## Funding

This work was supported by the National Institutes of Health (R01 AA025066).

## Declaration of competing interest

The authors declare that they have no known competing financial interests or personal relationships that could have appeared to influence the work reported in this paper.

## Acknowledgements

We wish to thank the patients and families who participated in this research.

## References

Andersson, J.L., Skare, S., Ashburner, J., 2003. How to correct susceptibility distortions in spin-echo echo-planar images: application to diffusion tensor imaging. Neuroimage 20, 870–888. https://doi.org/10.1016/S1053-8119(03)00336-7.

Andersson, J.L.R., Graham, M.S., Zsoldos, E., Sotiropoulos, S.N., 2016. Incorporating outlier detection and replacement into a non-parametric framework for movement and distortion correction of diffusion MR images. Neuroimage 141, 556–572. https://doi.org/10.1016/j.neuroimage.2016.06.058.

Aoki, Y., Cortese, S., Castellanos, F.X., 2018. Research Review: diffusion tensor imaging studies of attention-deficit/hyperactivity disorder: meta-analyses and reflections on head motion. JCPP (J. Child Psychol. Psychiatry) 59, 193–202. https://doi.org/10.1111/jcpp.12778.

Behrens, T.E., Woolrich, M.W., Jenkinson, M., Johansen-Berg, H., Nunes, R.G., Clare, S., Matthews, P.M., Brady, J.M., Smith, S.M., 2003. Characterization and propagation of uncertainty in diffusion-weighted MR imaging. Magn. Reson. Med. 50, 1077–1088. https://doi.org/10.1002/mrm.10609.

Bichenkov, E., Ellingson, J.S., 2001. Ethanol exerts different effects on myelin basic protein and 2',3'-cyclic nucleotide 3'-phosphodiesterase expression in

differentiating CG-4 oligodendrocytes. Brain Res Dev Brain Res 128, 9–16. https://doi.org/10.1016/s0165-3806(01)00142-0.
Bichenkov, E., Ellingson, J.S., 2002. Protein kinase C inhibitors counteract the ethanol effects on myelin basic protein expression in differentiating CG-4 oligodendrocytes. Brain Res Dev Brain Res 139, 29–38. https://doi.org/10.1016/s0165-3806(02)00512-6.
Bichenkov, E., Ellingson, J.S., 2009. Ethanol alters the expressions of c-Fos and myelin basic protein in differentiating oligodendrocytes. Alcohol 43, 627–634. https://doi.org/10.1016/j.alcohol.2009.09.026.
Carlsson, A., Waters, N., Carlsson, M.L., 1999. Neurotransmitter interactions in schizophrenia–therapeutic implications. Biol. Psychiatr. 46, 1388–1395. https://doi.org/10.1016/s0006-3223(99)00117-1.
CDC, 2004. Centers for Disease Control and Prevention. Fetal Alcohol Syndrome: Guidelines for Referral and Diagnosis. National Center on Birth Defects and Developmental Disabilities. Department of Health and Human Services.
Chen, L., Hu, X., Ouyang, L., He, N., Liao, Y., Liu, Q., Zhou, M., Wu, M., Huang, X., Gong, Q., 2016. A systematic review and meta-analysis of tract-based spatial statistics studies regarding attention-deficit/hyperactivity disorder. Neurosci. Biobehav. Rev. 68, 838–847. https://doi.org/10.1016/j.neubiorev.2016.07.022.
Chiappelli, F., Taylor, A.N., Espinosa de los Monteros, A., de Vellis, J., 1991. Fetal alcohol delays the developmental expression of myelin basic protein and transferrin in rat primary oligodendrocyte cultures. Int. J. Dev. Neurosci. 9, 67–75.
Colby, J.B., Smith, L., O'Connor, M.J., Bookheimer, S.Y., Van Horn, J.D., Sowell, E.R., 2012. White matter microstructural alterations in children with prenatal methamphetamine/polydrug exposure. Psychiatr. Res. 204, 140–148. https://doi.org/10.1016/j.pscychresns.2012.04.017.
Conners, K.C., 2008. Conners, third ed. Multi-Health Systems, Toronto.
Dale, A.M., Fischl, B., Sereno, M.I., 1999. Cortical surface-based analysis. I. Segmentation and surface reconstruction. Neuroimage 9, 179–194. https://doi.org/10.1006/nimg.1998.0395.
Dennis, M., Francis, D.J., Cirino, P.T., Schachar, R., Barnes, M.A., Fletcher, J.M., 2009. Why IQ is not a covariate in cognitive studies of neurodevelopmental disorders. J. Int. Neuropsychol. Soc. 15, 331–343. https://doi.org/10.1017/S1355617709090481.
Deoni, S.C., Dean 3rd, D.C., Remer, J., Dirks, H., O'Muircheartaigh, J., 2015. Cortical maturation and myelination in healthy toddlers and young children. Neuroimage 115, 147–161. https://doi.org/10.1016/j.neuroimage.2015.04.058.
Doig, J., McLennan, J.D., Gibbard, W.B., 2008. Medication effects on symptoms of attention-deficit/hyperactivity disorder in children with fetal alcohol spectrum disorder. J. Child Adolesc. Psychopharmacol. 18, 365–371. https://doi.org/10.1089/cap.2007.0121.
Esteban, O., Birman, D., Schaer, M., Koyejo, O.O., Poldrack, R.A., Gorgolewski, K.J., 2017. MRIQC: advancing the automatic prediction of image quality in MRI from unseen sites. PLoS One 12, e0184661. https://doi.org/10.1371/journal.pone.0184661.
Feldman, H.M., Yeatman, J.D., Lee, E.S., Barde, L.H., Gaman-Bean, S., 2010. Diffusion tensor imaging: a review for pediatric researchers and clinicians. J. Dev. Behav. Pediatr. 31, 346–356. https://doi.org/10.1097/DBP.0b013e3181dcaa8b.
Frankel, F., Paley, B., Marquardt, R., O'Connor, M., 2006. Stimulants, neuroleptics, and children's friendship training for children with fetal alcohol spectrum disorders. J. Child Adolesc. Psychopharmacol. 16, 777–789. https://doi.org/10.1089/cap.2006.16.777.
Fryer, S.L., McGee, C.L., Matt, G.E., Riley, E.P., Mattson, S.N., 2007. Evaluation of psychopathological conditions in children with heavy prenatal alcohol exposure. Pediatrics 119, e733–741. https://doi.org/10.1542/peds.2006-1606.
Ghazi Sherbaf, F., Aarabi, M.H., Hosein Yazdi, M., Haghshomar, M., 2019. White matter microstructure in fetal alcohol spectrum disorders: a systematic review of diffusion tensor imaging studies. Hum. Brain Mapp. 40, 1017–1036. https://doi.org/10.1002/hbm.24409.
Glasser, M.F., Sotiropoulos, S.N., Wilson, J.A., Coalson, T.S., Fischl, B., Andersson, J.L., Xu, J., Jbabdi, S., Webster, M., Polimeni, J.R., Van Essen, D.C., Jenkinson, M., Consortium, W.U.-M.H., 2013. The minimal preprocessing pipelines for the Human Connectome Project. Neuroimage 80, 105–124. https://doi.org/10.1016/j.neuroimage.2013.04.127.
Glasser, M.F., Van Essen, D.C., 2011. Mapping human cortical areas in vivo based on myelin content as revealed by T1- and T2-weighted MRI. J. Neurosci. 31, 11597–11616. https://doi.org/10.1523/JNEUROSCI.2180-11.2011.
Grydeland, H., Walhovd, K.B., Tamnes, C.K., Westlye, L.T., Fjell, A.M., 2013. Intracortical myelin links with performance variability across the human lifespan: results from T1- and T2-weighted MRI myelin mapping and diffusion tensor imaging. J. Neurosci. 33, 18618–18630. https://doi.org/10.1523/JNEUROSCI.2811-13.2013.
Hamilton, G.F., Hernandez, I.J., Krebs, C.P., Bucko, P.J., Rhodes, J.S., 2017. Neonatal alcohol exposure reduces number of parvalbumin-positive interneurons in the medial prefrontal cortex and impairs passive avoidance acquisition in mice deficits not rescued from exercise. Neuroscience 352, 52–63. https://doi.org/10.1016/j.neuroscience.2017.03.058.
Hannigan, J.H., Chiodo, L.M., Sokol, R.J., Janisse, J., Ager, J.W., Greenwald, M.K., Delaney-Black, V., 2010. A 14-year retrospective maternal report of alcohol consumption in pregnancy predicts pregnancy and teen outcomes. Alcohol 44, 583–594. https://doi.org/10.1016/j.alcohol.2009.03.003.
Henriquez-Henriquez, M., Acosta, M.T., Martinez, A.F., Velez, J.I., Lopera, F., Pineda, D., Palacio, J.D., Quiroga, T., Worgall, T.S., Deckelbaum, R.J., Mastronardi, C., Molina, B.S.G., Group, M.T.A.C., Arcos-Burgos, M., Muenke, M., 2020. Mutations in sphingolipid metabolism genes are associated with ADHD. Transl. Psychiatry 10, 231. https://doi.org/10.1038/s41398-020-00881-8.
Hoyme, H.E., Kalberg, W.O., Elliott, A.J., Blankenship, J., Buckley, D., Marais, A.S., Manning, M.A., Robinson, L.K., Adam, M.P., Abdul-Rahman, O., Jewett, T., Coles, C. D., Chambers, C., Jones, K.L., Adnams, C.M., Shah, P.E., Riley, E.P., Charness, M.E., Warren, K.R., May, P.A., 2016. Updated clinical guidelines for diagnosing fetal alcohol spectrum disorders. Pediatrics 138. https://doi.org/10.1542/peds.2015-4256.
Kaufman, J., Birmaher, B., Brent, D., Rao, U., Flynn, C., Moreci, P., Williamson, D., Ryan, N., 1997. Schedule for affective disorders and schizophrenia for school-age children-present and lifetime version (K-SADS-PL): initial reliability and validity data. J. Am. Acad. Child Adolesc. Psychiatry 36, 980–988. https://doi.org/10.1097/00004583-199707000-00021.
Khan, A., de Jong, L.A., Kamenski, M.E., Higa, K.K., Lucero, J.D., Young, J.W., Behrens, M.M., Powell, S.B., 2017. Adolescent GBR12909 exposure induces oxidative stress, disrupts parvalbumin-positive interneurons, and leads to hyperactivity and impulsivity in adult mice. Neuroscience 345, 166–175. https://doi.org/10.1016/j.neuroscience.2016.11.022.
Kilpatrick, L.A., Joshi, S.H., O'Neill, J., Kalender, G., Dillon, A., Best, K.M., Narr, K.L., Alger, J.R., Levitt, J.G., O'Connor, M.J., 2021. Cortical gyrification in children with attention deficit-hyperactivity disorder and prenatal alcohol exposure. Drug Alcohol Depend. 225, 108817. https://doi.org/10.1016/j.drugalcdep.2021.108817.
Kim, H., Ahrlund-Richter, S., Wang, X., Deisseroth, K., Carlen, M., 2016. Prefrontal parvalbumin neurons in control of attention. Cell 164, 208–218. https://doi.org/10.1016/j.cell.2015.11.038.
Kojima, H., Mineta-Kitajima, R., Saitoh-Harada, N., Kurihara, T., Takahashi, Y., Furudate, S., Shirataka, M., Nakamura, K., Tamai, Y., 1994. Prenatal ethanol exposure affects the activity and mRNA expression of neuronal membrane enzymes in rat offspring. Life Sci. 55, 1433–1442. https://doi.org/10.1016/0024-3205(94)00758-6.
Lesch, K.P., 2019. Editorial: can dysregulated myelination be linked to ADHD pathogenesis and persistence? JCPP (J. Child Psychol. Psychiatry) 60, 229–231. https://doi.org/10.1111/jcpp.13031.
Mastronardi, C.A., Pillai, E., Pineda, D.A., Martinez, A.F., Lopera, F., Velez, J.I., Palacio, J.D., Patel, H., Easteal, S., Acosta, M.T., Castellanos, F.X., Muenke, M., Arcos-Burgos, M., 2016. Linkage and association analysis of ADHD endophenotypes in extended and multigenerational pedigrees from a genetic isolate. Mol. Psychiatr. 21, 1434–1440. https://doi.org/10.1038/mp.2015.172.
Mazuir, E., Fricker, D., Sol-Foulon, N., 2021. Neuron-oligodendrocyte communication in myelination of cortical GABAergic cells. Life (Basel) 11. https://doi.org/10.3390/life11030216.
Micheva, K.D., Chang, E.F., Nana, A.L., Seeley, W.W., Ting, J.T., Cobbs, C., Lein, E., Smith, S.J., Weinberg, R.J., Madison, D.V., 2018. Distinctive structural and molecular features of myelinated inhibitory axons in human neocortex. eNeuro 5. https://doi.org/10.1523/ENEURO.0297-18.2018.
Micheva, K.D., Wolman, D., Mensh, B.D., Pax, E., Buchanan, J., Smith, S.J., Bock, D.D., 2016. A large fraction of neocortical myelin ensheathes axons of local inhibitory neurons. Elife 5. https://doi.org/10.7554/eLife.15784.
Moore, D.B., Quintero, M.A., Ruygrok, A.C., Walker, D.W., Heaton, M.B., 1998. Prenatal ethanol exposure reduces parvalbumin-immunoreactive GABAergic neuronal number in the adult rat cingulate cortex. Neurosci. Lett. 249, 25–28. https://doi.org/10.1016/s0304-3940(98)00378-4.
Mortamet, B., Bernstein, M.A., Jack, C.R., Gunter, J.L., Ward, C., Britson, P.J., Meuli, R., Thiran, J.P., Krueger, G., Alzheimer's Disease Neuroimaging, I, 2009. Automatic quality assessment in structural brain magnetic resonance imaging. Magn. Reson. Med. 62, 365–372. https://doi.org/10.1002/mrm.21992.
Natu, V.S., Gomez, J., Barnett, M., Jeska, B., Kirilina, E., Jaeger, C., Zhen, Z., Cox, S., Weiner, K.S., Weiskopf, N., Grill-Spector, K., 2018. Apparent thinning of visual cortex during childhood is associated with myelination, not pruning. bioRxiv 368274. https://doi.org/10.1101/368274.
Norbom, L.B., Rokicki, J., Alnaes, D., Kaufmann, T., Doan, N.T., Andreassen, O.A., Westlye, L.T., Tamnes, C.K., 2020. Maturation of cortical microstructure and cognitive development in childhood and adolescence: a T1w/T2w ratio MRI study. Hum. Brain Mapp. 41, 4676–4690. https://doi.org/10.1002/hbm.25149.
O'Connor, M.J., 2014. Mental Health outcomes associated with prenatal alcohol exposure: genetic and environmental factors. Curr Dev Disord Rep 1, 181–188. https://doi.org/10.1007/s40474-014-0021-7.
O'Connor, M.J., Portnoff, L.C., Lebsack-Coleman, M., Dipple, K.M., 2019. Suicide risk in adolescents with fetal alcohol spectrum disorders. Birth Defects Res 111, 822–828. https://doi.org/10.1002/bdr2.1465.
O'Malley, K.D., Nanson, J., 2002. Clinical implications of a link between fetal alcohol spectrum disorder and attention-deficit hyperactivity disorder. Can. J. Psychiatr. 47, 349–354. https://doi.org/10.1177/070674370204700405.
O'Neill, J., O'Connor, M.J., Kalender, G., Ly, R., Ng, A., Dillon, A., Narr, K.L., Loo, S.K., Alger, J.R., Levitt, J.G., 2021. Combining neuroimaging and behavior to discriminate children with attention deficit-hyperactivity disorder with and without prenatal alcohol exposure. Brain Imaging Behav. https://doi.org/10.1007/s11682-021-00477-w.
O'Neill, J., O'Connor, M.J., Yee, V., Ly, R., Narr, K., Alger, J.R., Levitt, J.G., 2019. Differential neuroimaging indices in prefrontal white matter in prenatal alcohol-associated ADHD versus idiopathic ADHD. Birth Defects Res 111, 797–811. https://doi.org/10.1002/bdr2.1460.
Oesterheld, J.R., Kofoed, L., Tervo, R., Fogas, B., Wilson, A., Fiechtner, H., 1998. Effectiveness of methylphenidate in Native American children with fetal alcohol syndrome and attention deficit/hyperactivity disorder: a controlled pilot study. J. Child Adolesc. Psychopharmacol. 8, 39–48. https://doi.org/10.1089/cap.1998.8.39.

Peadon, E., Rhys-Jones, B., Bower, C., Elliott, E.J., 2009. Systematic review of interventions for children with fetal alcohol spectrum disorders. BMC Pediatr. 9, 35. https://doi.org/10.1186/1471-2431-9-35.

Puentes-Rozo, P.J., Acosta-Lopez, J.E., Cervantes-Henriquez, M.L., Martinez-Banfi, M.L., Mejia-Segura, E., Sanchez-Rojas, M., Anaya-Romero, M.E., Acosta-Hoyos, A., Garcia-Llinas, G.A., Mastronardi, C.A., Pineda, D.A., Castellanos, F.X., Arcos-Burgos, M., Velez, J.I., 2019. Genetic variation underpinning ADHD risk in a caribbean community. Cells 8. https://doi.org/10.3390/cells8080907.

Quattlebaum, J.L., O'Connor, M.J., 2013. Higher functioning children with prenatal alcohol exposure: is there a specific neurocognitive profile? Child Neuropsychol. 19, 561–578. https://doi.org/10.1080/09297049.2012.713466.

Selten, M., van Bokhoven, H., Nadif Kasri, N., 2018. Inhibitory control of the excitatory/inhibitory balance in psychiatric disorders. F1000Res 7, 23. https://doi.org/10.12688/f1000research.12155.1.

Smiley, J.F., Saito, M., Bleiwas, C., Masiello, K., Ardekani, B., Guilfoyle, D.N., Gerum, S., Wilson, D.A., Vadasz, C., 2015. Selective reduction of cerebral cortex GABA neurons in a late gestation model of fetal alcohol spectrum disorder. Alcohol 49, 571–580. https://doi.org/10.1016/j.alcohol.2015.04.008.

Smith, S.M., 2002. Fast robust automated brain extraction. Hum. Brain Mapp. 17, 143–155. https://doi.org/10.1002/hbm.10062.

Smith, S.M., Jenkinson, M., Johansen-Berg, H., Rueckert, D., Nichols, T.E., Mackay, C.E., Watkins, K.E., Ciccarelli, O., Cader, M.Z., Matthews, P.M., Behrens, T.E., 2006. Tract-based spatial statistics: voxelwise analysis of multi-subject diffusion data. Neuroimage 31, 1487–1505. https://doi.org/10.1016/j.neuroimage.2006.02.024.

Smith, S.M., Nichols, T.E., 2009. Threshold-free cluster enhancement: addressing problems of smoothing, threshold dependence and localisation in cluster inference. Neuroimage 44, 83–98. https://doi.org/10.1016/j.neuroimage.2008.03.061.

Snyder, J., Nanson, J., Snyder, R., Block, G., 1997. A study of stimulant medication in children with FAS. In: Streissguth, A., Kanter, J. (Eds.), Overcoming and Preventing Secondary Disabilities in Fetal Alcohol Syndrome and Fetal Alcohol Effects. University of Washington Press, Seattle, WA, pp. 64–77.

Stedehouder, J., Couey, J.J., Brizee, D., Hosseini, B., Slotman, J.A., Dirven, C.M.F., Shpak, G., Houtsmuller, A.B., Kushner, S.A., 2017. Fast-spiking parvalbumin interneurons are frequently myelinated in the cerebral cortex of mice and humans. Cerebr. Cortex 27, 5001–5013. https://doi.org/10.1093/cercor/bhx203.

Taylor, P.A., Jacobson, S.W., van der Kouwe, A., Molteno, C.D., Chen, G., Wintermark, P., Alhamud, A., Jacobson, J.L., Meintjes, E.M., 2015. A DTI-based tractography study of effects on brain structure associated with prenatal alcohol exposure in newborns. Hum. Brain Mapp. 36, 170–186. https://doi.org/10.1002/hbm.22620.

Tomassy, G.S., Berger, D.R., Chen, H.H., Kasthuri, N., Hayworth, K.J., Vercelli, A., Seung, H.S., Lichtman, J.W., Arlotta, P., 2014. Distinct profiles of myelin distribution along single axons of pyramidal neurons in the neocortex. Science 344, 319–324. https://doi.org/10.1126/science.1249766.

Townsend, L., Kobak, K., Kearney, C., Milham, M., Andreotti, C., Escalera, J., Alexander, L., Gill, M.K., Birmaher, B., Sylvester, R., Rice, D., Deep, A., Kaufman, J., 2020. Development of three web-based computerized versions of the kiddie Schedule for affective disorders and schizophrenia child psychiatric diagnostic interview: preliminary validity data. J. Am. Acad. Child Adolesc. Psychiatry 59, 309–325. https://doi.org/10.1016/j.jaac.2019.05.009.

Wechsler, D., 2011. Wechsler Abbreviated Scale of Intelligence, second ed. NCS Pearson, San Antonio (WASI-II).

Winkler, A.M., Ridgway, G.R., Webster, M.A., Smith, S.M., Nichols, T.E., 2014. Permutation inference for the general linear model. Neuroimage 92, 381–397. https://doi.org/10.1016/j.neuroimage.2014.01.060.

Winkler, A.M., Webster, M.A., Brooks, J.C., Tracey, I., Smith, S.M., Nichols, T.E., 2016. Non-parametric combination and related permutation tests for neuroimaging. Hum. Brain Mapp. 37, 1486–1511. https://doi.org/10.1002/hbm.23115.

Yakovlev, P.L., Lecours, A.R., 1967. The myelogenetic cycles of regional maturation of the brain. In: M, A. (Ed.), Resional Development of the Brain in Early Life. Blackwell, Oxford, pp. 3–70.